



Progressively cooler, drier interglacials in southern Russia through the Quaternary: Evidence from the Sea of Azov region

A.A. Velichko^a, N.R. Catto^{b,*}, M. Yu Kononov^a, T.D. Morozova^a, E. Yu Novenko^a, P.G. Panin^a, G. Ya Ryskov^a, V.V. Semenov^a, S.N. Timireva^a, V.V. Titov^a, A.S. Tesakov^a

^a*Institute of Palaeogeography, Russian Academy of Sciences, Moscow, Russian Federation*

^b*Department of Geography, Memorial University of Newfoundland, St. John's, NL Canada, A1B 3X9*

Abstract

Loess-palaeosol exposures along Taganrog Bay, Sea of Azov, in southern Russia, reveal a complex succession of Quaternary palaeoenvironments over the past 0.7 million years. The deposits overlie marine sediments of Tiraspolian (Cromerian) age. At the key section of Semibalki-1, four palaeosol complexes are identified within the series. The earliest palaeosol complex in the Semibalki-1 section is correlated with the late Muchkap Interglacial (the Vorona palaeosol). The soil type resembled modern subtropical Mediterranean region soils. The later Middle Pleistocene palaeosols bear evidence of soil-forming processes typical of various temperate zone environments, with a gradual transition to increasingly cooler, drier conditions. Soils suggesting transitional development between kastnozems and chernozems developed during the Likhvin Interglacial (Inzhavino PC). PC 2 (Kamenka Interglacial) is typified by eluviated Luvic Chernozemic soils, possibly formed under prairie parkland conditions. Finally, the Mikulino Interglacial of the Late Pleistocene (Mezin PC) is represented by chernozems similar to the modern (Holocene) soils of the region, but showing enhanced podzolization and fewer seasonal frost features.

A succession of environmental changes has been traced in the study region, from semi-humid subtropical environments at the end of the Early Pleistocene to prairie environments, then to boreal-mild temperate during the Middle Pleistocene, and finally towards landscapes with typical steppe soils in the Late Pleistocene and Holocene. The sequence indicates that moisture supply and temperatures during successive interglacials shifted progressively towards increasingly cooler, somewhat drier climates, influencing soil formation.

© 2008 Elsevier Ltd and INQUA. All rights reserved.

1. Introduction

The Azov Sea coast has long commanded the attention of many investigators, as it furnishes an opportunity to gain a better understanding of the interrelation between marine and continental deposits in southern European Russia. Different series of marine, lagoonal, and fluvial sediments and overlying subaerial formations (including palaeosol horizons) have been described and discussed in numerous papers by Lisitsyn (1925), Moskvitin (1932), Gromov (1933) and many others (Khokhlovkina, 1940; Lebedeva, 1965; Agadjanian et al., 1972; Bolikhovskaya and Dobrodeev, 1972; Velichko et al., 1973, 2006a,b; Dodonov et al., 2005).

This contribution presents some results of research on the project “Historical reconstruction of the chernozem steppe formation in arid zones”, part of the Russian Academy of Sciences Program (Earth Science Division), “Monitoring technology development, ecosystem modeling and forecast in studies of natural resources in arid environments”, under the direction of G.G. Matishov. The project is aimed at multi-disciplinary studies of loess-palaeosol series which contain several fossil soils dated from early Quaternary to Holocene. This approach provides a means for estimating environmental changes, including variations of temperature and water supply, soil formation processes, and degree of aridity in southern European Russia, through the Quaternary glacial and interglacial epochs to the present day.

One of the most thoroughly studied key sections is Semibalki-1, located on the southern coast of Taganrog

*Corresponding author. Tel.: +1 709 737 8413; fax: +1 709 737 3119.

E-mail address: ncatto@mun.ca (N.R. Catto).

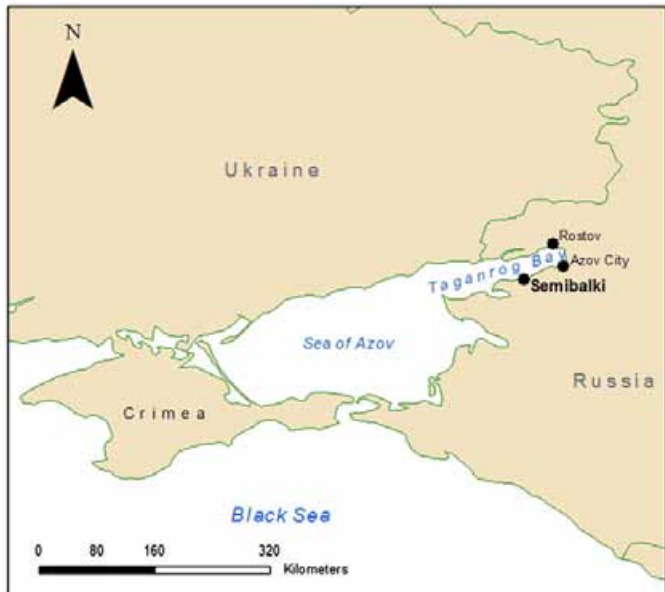


Fig. 1. Location of Semibalki-1 exposure.

Bay (Fig. 1). The major consideration in choosing this section as an object of multi-disciplinary studies was a wide chronological range of the exposed subaerial horizons and the possibility of correlation from the continental loess-palaeosol series to marine-lagoonal sediments of Tiraspolian (Cromerian) age. This offered a way of evaluating environmental and climate changes within the Sea of Azov area from the latest Early Pleistocene through the Holocene, about 0.7 million years.

The Semibalki-1 section is about 30 km west of Azov city, at the eastern margin of the Semibalki village. A coastal scarp cuts across a terrace surface 35 m high. A loess-palaeosol series about 15 m thick is exposed, underlain with marine (lagoonal) sands. Lebedeva (1965) established that the latter are of Tiraspolian (Cromerian) age.

During field studies, attention was focused on the palaeosols. Stratigraphic positions were established on the basis of their relationship with the underlying lagoonal sediments and through stratigraphic comparison with previously dated palaeosols known from regions farther north on the East European Plain (e.g. Velichko, 1990; Velichko et al., 1999, 2005, 2006a, b; Dlussky, 2001, 2007; Little, 2002; Little et al., 2002; Puterbough et al., 2005). Analysis of Semibalki and adjacent sections completes a north-south transect of loess-palaeosol assemblages extending from the Moscow region to the Sea of Azov.

2. Stratigraphy of Semibalki-1

The subaerial loess-palaeosol series exposed at the Semibalki-1 section has been described and sampled in a number of exposures along the coastal scarp, parts of a continuously exposed section (Figs. 2 and 3). A summarized description of the composite section is presented here,

with cleaned exposures numbered from youngest to oldest. All colour designations are standard Munsell values, taken from moist, fresh samples.

Exposure 1 (Fig. 2):

1. *A humic horizon of the modern Holocene Chernozem soil*: Sandy loam; 10YR 3/1 (dark grey); granular structure; gradational lower contact; thickness 0.80 m, cumulative thickness 0.80 m.
2. *Transitional A/B horizon*: Loam-to-sandy loam; 10YR 5/2 (pale yellow-grey); prismatic to fine blocky structure; gradational lower contact; thickness 0.70 m, cumulative thickness 1.50 m.
3. *Bca horizon*: Loam to sandy loam; 10YR 4/3 (yellowish-brown); porous; prismatic structure; carbonate accumulations; indistinct lower contact; thickness 0.50 m, cumulative thickness 2.00 m.
4. *BC horizon, pedogenically modified loess*: Sandy loam; 10YR 6/4 (pale yellow, with brownish hue); prismatic to medium angular blocky structure; almost completely devoid of carbonates; krotovinas 8–15 cm in diameter; gradational lower contact; thickness 0.65 m, cumulative thickness 2.65 m.
5. *Valdai loess*: Fine sandy silt loam; 10YR 6/4 (grayish-yellow); fine prismatic structure; fine pores; weakly calcareous; sharp lower contact; thickness 2.25 m, cumulative thickness 4.90 m.

Exposure 2: 1.5 m to the west of exposure 1 (Fig. 2).
Mezin Palaeosol complex (PC 1)

6. *Upper humified horizon; Krutitsa interstadial phase of the Mezin soil complex*: Loam; 10 YR 5/4 (brown, with weak grey hue); well-developed fine columnar prismatic structure; compact, firm, and cohesive; isolated fine carbonate crystals (2–3 mm) in pores; gradational lower contact; thickness 0.47 m, cumulative thickness 5.37 m.
7. *Lower humic horizon; Salyn phase of the Mezin soil complex, corresponding to the Mikulino Interglacial*: Loam; 10 YR 4/4 (grey-brown); well-developed fine columnar prismatic structure; compact, firm, and cohesive; upper part abounds in fine-grained (powdery) carbonates concentrated in macropores (root channels) 2–4 mm in diameter; decreasing carbonate concentrations below 0.30 m thickness; gradational lower contact; thickness 0.63 m, cumulative thickness 6.00 m
8. *AB horizon*: Loam; 10 YR 4/4 (grey-brown); medium prismatic structure; isolated powdery carbonate crystals; krotovinas of burrowing animals (3–5 cm diameter); distinct lower contact; thickness 0.45 m, cumulative thickness 6.45 m.
9. *Bca horizon*: Loam; 10 YR 4/3 (grayish-brown, with a weak yellowish hue); prismatic structure; abundant carbonate weakly lithified nodules and concentrations (“byeloglezka”), 0.5–0.8 cm diameter; krotovinas infilled with material from the overlying soil horizon (unit 8) to 5 cm diameter; distinct lower contact, but without evidence of erosion; thickness 0.77 m, cumulative thickness 7.22 m.

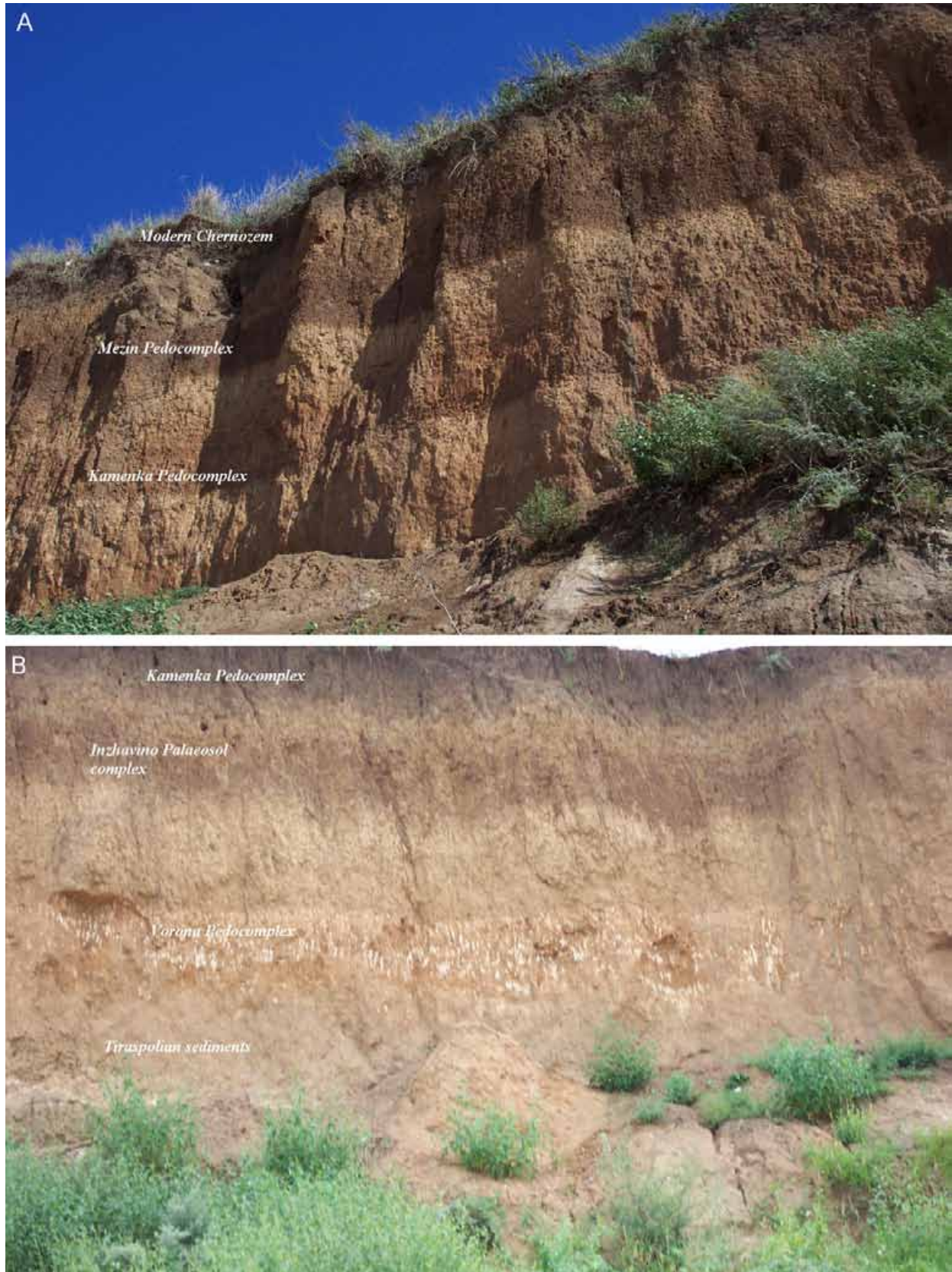


Fig. 2. (A) Uppermost part of the Semibalki-1 exposure. Visible are the MIS 1 Holocene Chernozem (units 1-3); MIS 2-4 Valdai loess (units 4 and 5); MIS 5 Mezin palaeosol complex (units 6-8); MIS 6 pedogenically modified loess (unit 9); and MIS 7 Kamenka palaeosol complex (units 10-11). (B) Lowermost part of the Semibalki-1 exposure. Visible below the modern Holocene Chernozem are the lower part of the Kamenka palaeosol complex (units 12-13), the Inzhavino palaeosol complex (units 14-17), the Vorona palaeosol complex (units 18-20), and the upper part of the Tiraspolian sediments (units 21-22).

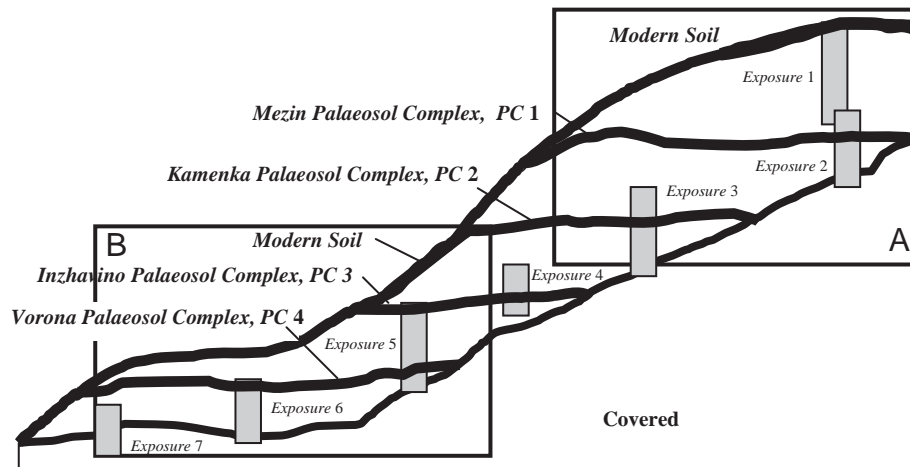


Fig. 3. Schematic diagram of the Semibalki-1 section. Location of individual exposures (as indicated in the description) is shown by grey boxes.

Numerous vertical veins (3–5 cm wide and spaced 20–30 cm apart) extend from the upper contact into the underlying unit 10. Boundaries are slightly wavy. The veins are infilled with brownish-yellow loam with indistinct horizontal lamination.

Kamenka Palaeosol complex (PC 2)

10. *Am* horizon: Loam; 10 YR 4/3 (grayish-brown); fine prismatic structure; carbonate present only as vertical inclusions arranged as veinlets 4–8 mm wide, along fossil plant roots; krotovinas to 12 × 15 cm², filled with material from layer 8; numerous vertical veins penetrate to the lower portion of the layer 10 and below; distinct lower contact; thickness 0.84 m; cumulative thickness 8.06 m.

Exposure 3: 7.5 m to the east of exposure 2.

11. *Bm* horizon: Loam; 10 YR 3/3 (dark brown); granular structure; compact and firm; scattered carbonate concentrations (“byeloglazka”) due to carbonate migration from the overlying layer; fine vertical veins extending from units 9 and 10; distinct lower contact; thickness 0.50 m, cumulative thickness 8.56 m.
12. *Bca* horizon: Loam; 10 YR 4/4 (brown); weak prismatic to granular structure; compact; abundant carbonate inclusions (“byeloglazka” type) in upper 0.50 m, but reduced in lower 0.25 m; krotovinas 5–7 cm in diameter; vertical veinlets 2–4 cm wide filled with material from the overlying horizons, forming the continuation of structures extending downwards from unit 9; gradational lower contact; thickness 0.82 m, cumulative thickness 9.38 m.

Exposure 4: 1.5 m to the east of exposure 3.

13. *Lower B* horizon: Clayey loam to clay; 10 YR 5/5 (light brown), grading downwards to 10 YR 4/4 (brown); granular-to-weak fine blocky; compact; manganese oxide staining on block surfaces; distinct lower contact; thickness 0.47 m, cumulative thickness 9.85 m.

Inzhavino Palaeosol complex (PC 3), attributed to the Likhvin Interglacial (Fig. 4)

14. *A* horizon: Sandy loam, humic; 10 YR 4/4 (brown); strong medium to coarse blocky structure; vertical



Fig. 4. Inzhavino palaeosol complex, units 14–16, showing post-depositional vertical fracturing and Krotovina development.

fissures 4–5 cm wide separating blocks are infilled with material from unit 13; manganese oxide staining on block surfaces; gradational lower contact; thickness 0.50 m, cumulative thickness 10.35 m.

15. *AB horizon*: Loam, humic; 10YR 3/3 (dark grey-brown); fine blocky structure; compact; split by vertical fractures into columns, increasing in width from 10–15 cm in the upper part of the layer to 30–40 cm towards its base. The width of inter-block infilled fractures varies from 3–5 to 8–12 cm, and they are filled with grey-yellowish loam, resembling that of the overlying layer; colouring due to humus darkens downwards. Krotovinas 5 × 8 and 5 × 10 cm² in dimensions filled with mixed material (from blocks and fissures) occur within the lower 0.3 m of the layer; gradational lower contact; thickness 0.75 m, cumulative thickness 11.10 m.
16. *AB horizon*: Loam to clayey loam, humic; 10 YR 3/3 (dark grey-brown); fine blocky to granular structure; distinct iron oxide films on ped facets; individual columns (between vertical fissures) widen to 60–65 cm; fissures are reduced in width to 5–7 cm; gradational lower contact; thickness 0.35 m, cumulative thickness 11.40 m.

Exposure 5: 1.5 m to the east of Exposure 4.

17. *B horizon*: Loam to sandy loam; 10 YR 4/4 to 10 YR 3/4 (brown to brownish grey); granular-to-weak fine blocky structure; fine silty carbonates in pores; isolated krotovinas (5–10 cm dimensions) filled with material from humus horizon; numerous thin (5–10 mm) sub-vertical veinlets penetrate into unit 17 from the overlying layer; distinct lower contact; thickness 0.30 m, cumulative thickness 11.85 m.

Vorona Palaeosol complex (PC 4), attributed to the Muchkap Interglacial (Fig. 5).

18. *A horizon*: Sandy loam; 7.5 YR 5/8 (red-brown); weak fine blocky to granular structure; friable, non-cohesive; fine porosity; carbonate inclusions (“byeloglazka”); krotovinas (5–10 cm) filled with humus material from the above-lying soil; trace structures of small burrowing animals (10–15 mm) filled with dark-grey organic matter; gradational contact; thickness 0.88 m, cumulative thickness 12.73 m.

Exposure 6: 10 m to the east of Exposure 5.

19. *AB horizon*: Loam; 7.5 YR 4/3 (reddish brown); weak fine blocky to granular structure; friable, non-cohesive; fine porosity; rare carbonate inclusions (“byeloglazka”); scattered krotovinas (5 cm) filled with materials presumably from the overlying layer; gradational lower contact; thickness 0.47 m, cumulative thickness 13.20 m.
20. *Bca horizon*: Sandy loam-to-loam; 5YR 4/6 (light yellow-brown); very weak fine blocky to granular structure; friable, non-cohesive; rich in fine carbonates; some “byeloglazka” inclusions; carbonate content decreases with depth; gradational lower contact; thickness 0.65 m, cumulative thickness 13.85 m.
21. *BC horizon*: Sandy loam; 7.5 YR 5/4 (grayish-yellow); very weak fine blocky to granular structure; friable, non-cohesive; carbonate “byeloglazka” inclusions; small manganese oxide crystals; krotovinas with



Fig. 5. Vorona palaeosol complex, units 18–20, showing abundant carbonate inclusions and krotovinas. The complex shows the effects of enhanced chemical weathering (calcareous concretions, overprinting cutan development, and iron staining).

5–15 cm dimensions. In the lower part (within 25 cm above base) the layer becomes gradually lighter, with isolated lenses of light grey fine sand. The increase in sand content is noticeable from the cumulative thickness of 14–14.5 m, indicating that the soil developed on the underlying lagoonal sediments; gradational lower contact; thickness 1.05 m, cumulative thickness 14.90 m.

Tiraspolian (Cromerian) sand (Fig. 6).

22. *Fine sand*: 10 YR 7/3 (light grey with a slight greenish hue); horizontally stratified, with fine cross-lamination within horizontal beds; subvertical root channels penetrate from the overlying unit; krotovinas with 5–15 cm dimensions; thickness in exposure 6 is 0.25 m, cumulative thickness 15.15 m.

Exposure 7: 6 m to the east of Exposure 6.

Unit 22: To a depth of 1.3 m from the upper contact, the layer is similar to that described in Exposure 6 in structure (horizontal bedding and cross-lamination) and the presence of krotovinas. From 1.3 m downward



Fig. 6. Tiraspolian sediments of unit 22, showing characteristic ripple structures.

to 1.6 m, horizontal strata and wave ripple laminae become thinner (horizontal strata 0.5–1.0 cm thickness) and more frequent. From 1.6 m downward, the bedding becomes less pronounced and practically disappears at 2 m. Here, unit 22 is structureless fine sand. The base of the exposed layer is 6–8 m above sea level. Total cumulative thickness is 18 m.

3. Analytical results

Analyses of samples from Semibalki-1 included: granulometric (pipette) determinations; carbonate content; humus and organic carbon content (using the Tyurin method); palaeosol micromorphology (studied in thin sections); pollen assemblages; small mammal fauna; sand quartz grain microscopy; magnetic susceptibility; and oxygen isotope determinations. Selected data are presented in Fig. 7.

3.1. Granulometry

Coarse silt (0.05–0.01 mm) and clay (>0.001 mm) are dominant fractions in the Semibalki-1 section from the top to a depth of ~12.5 m (units 1–19). From unit 20

downward, fine sand (0.25–0.05 mm) prevails. The sand proportion in the upper part is negligible (no more than 1%), with the exception of the uppermost part of the modern chernozem, where fine and medium-grain sand content reaches 10%.

The proportion of the loessial (0.05–0.01 mm) fraction reaches its maximum (34–40%) in layers 1–5, dated to the late Quaternary (MIS 1–4). From the Mezin palaeosol complex downward (layers 6–18) it ranges from 20% to 30%. In the Vorona palaeosol complex and the underlying Tiraspolian sediment at the base of the section (layers 19–22), the sand fraction is dominant and the silt fraction is no more than 2–3%.

Clay (<0.001 mm) content is rather high, reaching 35–45%, in the Salyn (Mezin), Kamenka, Inzhavino, and Vorona palaeosols in particular. It drops conspicuously in the lagoonal sediments.

3.2. Humus content

Except for the modern chernozem, where humus content amounts to 1–2.4%, all the palaeosols and intervening layers are depleted in humus (0.4–0.1%) (Fig. 7). This phenomenon is attributed to diagenetic transformation of

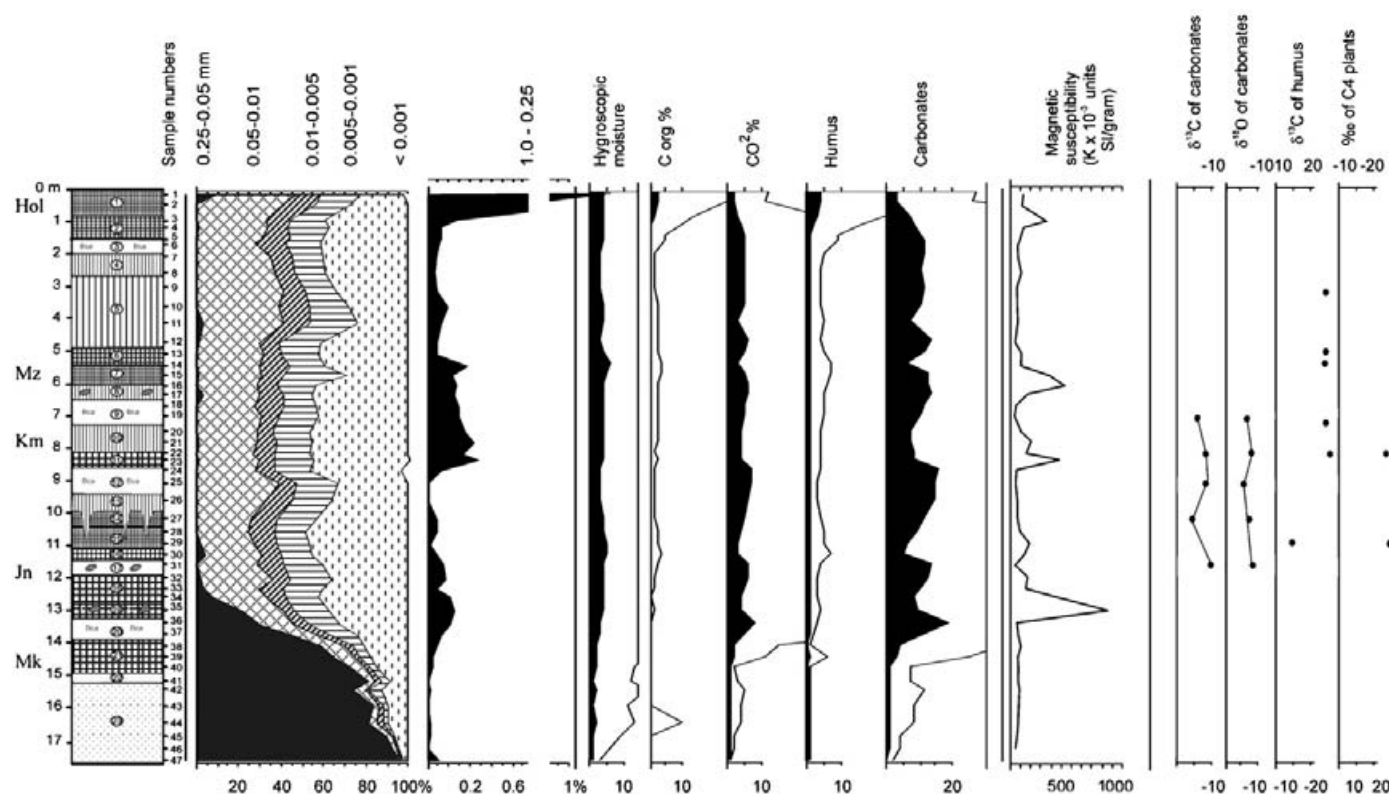


Fig. 7. Results of analyses (lithology, chemical composition, magnetic susceptibility, oxygen, and carbon isotopes). Soil horizons and palaeosol complexes in the sequence are denoted as follows: Hol—the Holocene soil, Mz—Mezin PC (PC 1), Km—Kamenka PC (PC 2), In—Inzhavino PC (PC 3), Vr—Vorona PC (PC 4). Explanations: 1—loess; 2—humus horizons (A) varying in colour intensity: 2a—darker, 2b—lighter; 3—transitional horizons (A/B); 4—horizons B: 4a—with carbonates, 4b—with krotovinas; 5—lagoonal (liman)-marine sand.

the buried soils (Morozova, 1981). Humus content is relatively low even in dark grey and dark brown horizons.

3.3. Carbonate content

The entire succession, with the exception of the basal marine sediments, contains calcium carbonate in abundance. Carbonate concentrations are indicative of the presence of illuvial calcareous horizons in the palaeosols. Secondary carbonates are commonly accumulated at the top of humus horizons, the latter forming a kind of impediment to carbonate translocation at the boundary with overlying layers. Such horizons of carbonate accumulation are found in all the palaeosols exposed in the Semibalki-1 section.

4. Paleopedological characteristics

Palaeosol genesis determinations were based on field descriptions of palaeosol genetic profiles, as well as on micromorphological studies of thin sections prepared from undisturbed oriented samples. The upper palaeosol complex (PC-1, units 6–9) described in the Semibalki-1 section occurs at a depth of ~5 m, directly under the 2.25 m loess layer (unit 4). The main phase of the palaeosol complex development correlates with the Mikulino Interglacial (see e.g. Velichko et al., 2006a).

4.1. PC-1, Mezin palaeosol complex (Mikulino interglacial), units 6–9

The palaeosol has a genetic profile including upper and lower humic horizons, a transitional AB horizon with krotovinas, and a Bca horizon. The palaeosol complex is broken into elongated blocks by vertical fissures filled with loess material from the overlying unit.

The upper humic horizon (unit 6) was probably formed during the concluding phase of soil formation and may correspond to the Krutitsa interstadial of the early Valdai glacial epoch (MIS 5.1). The micromorphological data indicates that the upper humic horizon has an open, loose microstructure and is well aggregated. The first-order aggregates are of various shapes, separated by irregular pores. The matrix groundmass is silty-plasmic. There are scattered aggregates with dark grey plasma heavily impregnated with humus. The groundmass contains numerous dark grey to black concentrations of humus flakes (Fig. 8A).

The lower humic horizon (unit 7) has aggregates with highly variable shapes. The matrix groundmass is silty-plasmic, with isotropic dark grey clayey-humus plasma. Scattered gypsum crystals are present.

The Bca horizon (unit 9) is heavily impregnated with fine calcite, with carbonates deposited in pores. Calcium carbonate content amounts to 11–13%. Dark ferruginous

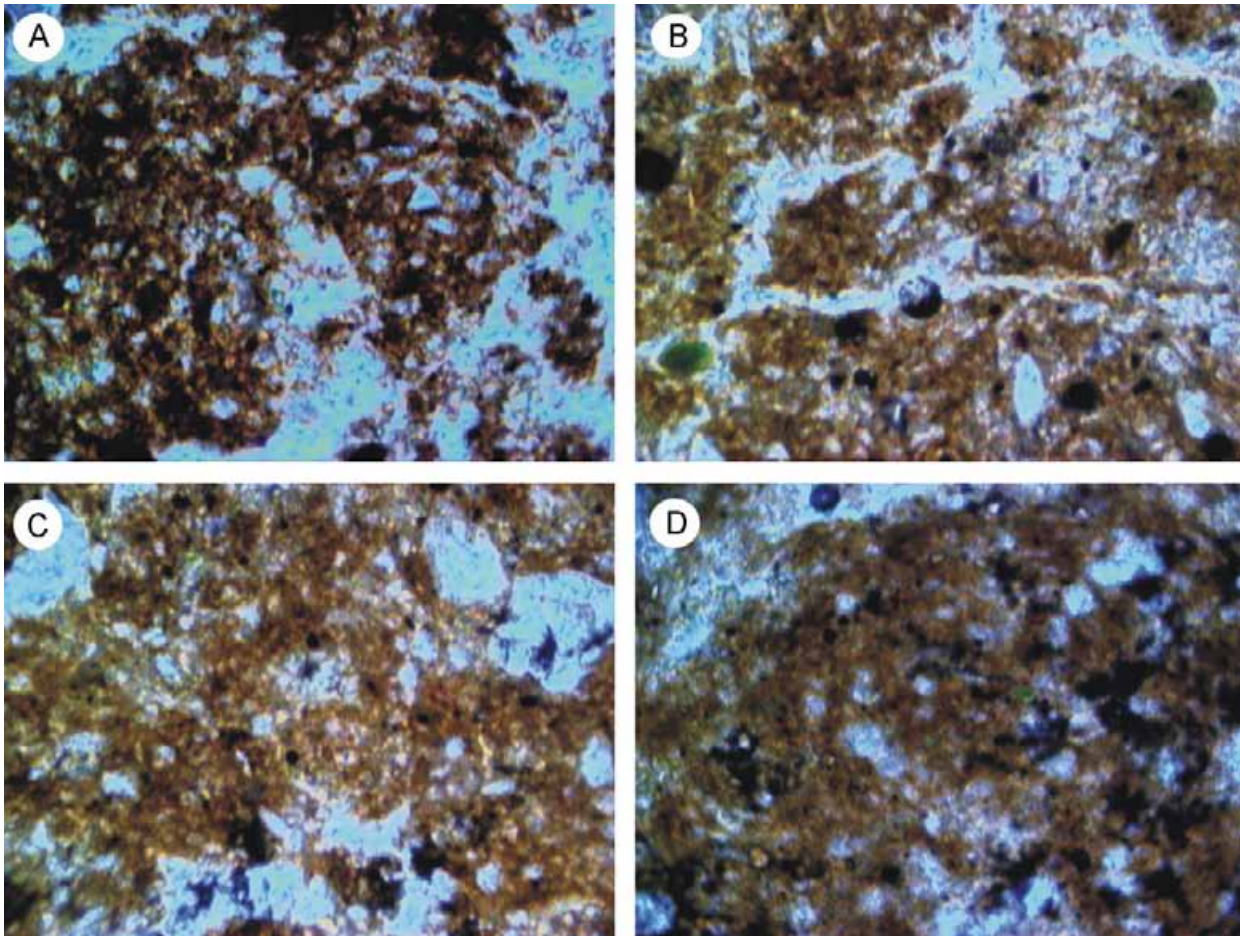


Fig. 8. Microstructure of palaeosol complexes: (A) Chernozem of the Mikulino Interglacial: humus horizon with complex aggregates; pores between aggregates are well developed. (B) Eluviated soil of the Kamenka Interglacial, showing Chernozemic characteristics, with overprints of eluviation: block microstructure of Am horizon; humic-clayey plasma, at places—humic-ferruginous plasma; pores between aggregates. (C) Humus horizon of the eluviated Inzhavino palaeosol, showing mixed Kastenzemic and Chernozemic characteristics: well-aggregated clayey-humic plasma, ferruginous aggregates in the matrix. (D) Humus-ferruginous aggregated matrix of the semi-humid subtropical Vorona palaeosol (the Muchkap Interglacial): dark brown and black newly formed aggregations of iron oxides.

neof ormations, opaque, with crystalline luster in reflected light are abundant.

Humus content is at its maximum (0.69%) near the base of the lower humic horizon. The palaeosol features an isohumus profile which is typical of a chernozem. Below the humic-rich horizon, the humus content decreases gradually towards the base of profile.

Judging from the soil morphology and micromorphology, the palaeosol may be interpreted as chernozemic. At the later stage of the soil formation, the sedimentation rate increased and humus accumulation was reduced. A Bca horizon of calcium carbonate accumulation was developed. Higher carbonate content in the upper part of the lower humic horizon (~11%) suggests secondary (post-burial) enrichment in carbonates. The gypsum presence in the central part of the humus horizon (not usually found in modern soils) may be also secondary. Bioturbations (traces of earthworm activity) are well pronounced. Krotovinas are found in abundance.

Noteworthy is a high proportion of clay (<0.001 mm), up to 45%, with a negligible presence of sand. The loess fraction (0.05–0.01 mm) varies from 20% to 30%.

4.2. PC-2, Kamenka palaeosol complex (Kamenka Interglacial) (units 10–13)

The second palaeosol is found at a depth of ~8 m. The profile consists of an Am horizon (unit 10), Bm (unit 11), Bca (unit 12), and lower B horizons (unit 13). Humus is regularly distributed through the palaeosol, its content gradually decreasing towards the base (isohumus profile), from a maximum of 0.43% in the Am horizon.

Micromorphologically, the Am horizon has a blocky structure, with individual blocks up to 1–1.2 mm. There are smaller blocky aggregates within the blocks, separated by pores and fissures. The matrix groundmass is silty-plasmic, with a brown, humus-clayey, and possibly humus-ferruginous-clayey plasma. In reflected light, it has a slightly

brownish hue due to the presence of iron hydroxides. There are clusters of dark brown amorphous iron hydroxides. The material is impregnated with micritic calcite. Microcrystalline gypsum is also present. The B-fabric is speckled (Fig. 8B).

The Bm horizon microstructure is blocky, with smaller rounded aggregates (probably of biogenic origin) within blocks. The matrix groundmass is silty-plasmic. The plasma shows speckled and weakly pronounced striated B-fabric. There are local segregations of clayey matter featuring undulatory extinction under crossed nicols. In reflected light, they are red-brown due to dispersed iron hydroxides. There are small isolated areas impregnated with micritic calcite. The Bca horizon is aggregated. Spherical clusters of iron hydroxides appear orange in reflected light.

The peak of calcium carbonate content in the upper part of the profile may be indicative of secondary accumulation. The fragmentary microstructure, brownish colouring of clay matter (due to the presence of dispersed iron), the hydroxides present as loose clusters in the matrix, isohumus profile, and striated B-fabric all suggest that clay formation and diagenesis participated in soil development.

Eluviation was evidently a major process affecting the entire palaeosol complex, with multiple generations of eluviation overprinted. The degree of alteration makes classification difficult. The complex shows elements of both prairie-parkland luvisols, developed along the deciduous forest/prairie border, and chernozemic soils. In total, the complex is considered to represent chernozemic soils that have been subject to extensive eluviation.

4.3. PC-3, Inzhavino palaeosol complex (Likhvin Interglacial) (units 14–17)

The third palaeosol complex is a polygenetic formation, consisting of at least two palaeosols. The final phase of soil formation is recorded in the humic A horizon (unit 14), distinct for its complicated structure. Vertical fissures have split it into elongated blocks. The width of individual blocks increases with depth from 10–15 to 30–40 cm. Colours darken from light to dark grey towards the lower part due to higher humus content (increasing downwards from 0.36% to 0.45%).

Samples from the lower horizon of this soil (unit 15), when studied in thin sections, are bright brown in reflected light. Microstructure varies from blocky to aggregated (within blocks). The aggregates are rounded, and some are of biogenic nature. The groundmass matrix is silty-plasmic, with humus-ferruginous-clayey plasma. There are abundant flaky clusters in the groundmass, as well as concentrations of dark grey to black iron and manganese hydroxides. The B-fabric is weakly pronounced and speckled to fibrous. There are brown spherical concentrations of clay, with concentric striated B-fabric. The groundmass is impregnated with silty carbonates. CaCO₃ content decreases downwards (11–6.5%).

The palaeosol attributable to the main phase of soil formation (units 16–17) features an A-Bca profile (with krotovinas), darker grey colour, with brownish hue, and well-developed structure. Micromorphologically, it is distinct for its loose-aggregated structure and unevenly distributed colour. The B-fabric is speckled or speckled-striated (Fig. 8C). The humus content increases with depth. Impregnation with micritic calcite is evident, and there are numerous secondary iron oxide concentrations. Humus content here is very high (0.71%), which may reflect the leading role of humus accumulation processes in the soil formation. Humus is evenly distributed in an isohumus profile. The Bca horizon abounds in krotovinas.

The palaeosol of the main phase development was marked by humus accumulation processes. This soil has dominantly chernozemic characteristics. However, the complex also shows signs of kastenozem development, especially in the upper part. The humus accumulation rate decreased towards the final stage, and clay formation and ferrugination became dominant. Taken as a whole, the complex represents a transition from chernozemic to kastenozemic soil development, suggesting a change over time towards warmer, perhaps more humid conditions.

4.4. PC-4, Vorona palaeosol complex (Muchkap Interglacial) (units 18–20)

This complex occurs directly under the krotovina horizon of the Inzhavino PC. The genetic profile includes A, AB, and Bca horizons.

The upper part of the humic A horizon is brown, and abounds in krotovinas (penetrating from the overlying palaeosol) and carbonate concretions. The lower 40 cm of unit 18 are darker, with reddish hue. Micromorphologically, the palaeosol is compact, with the soil mass divided into blocks. The groundmass is silty-ferruginous-clayey. The B-fabric is predominantly speckled and striated, especially near fissures. Abundant powdery carbonates impregnate the groundmass. There are rounded brown clayey nodules (0.5 mm), showing undulatory extinction, that could represent the remains of illuviation cutans.

Diagenetic iron hydroxide is present in various forms (black, isotropic). Near the base of profile, the microstructure is less compact and aggregated. The sample is heavily impregnated with micritic carbonates. Some sand grains are present, as well as flaky concentrations of humus (Fig. 8D).

The Bca horizon shows loose-aggregated microstructure, locally impregnated with micritic calcite, with scattered gypsum inclusions. Sand is present in small amounts. Sand and carbonate content is noticeably higher in samples from the base of the palaeosol complex. The palaeosol displays properties not unlike to those of modern subtropical soils (cinnamonic or transitional subtypes) formed in semi-humid environments.

5. Morphoscopy of quartz sand grains

Morphoscopy is of great use in determination of sediment genesis. As well, in the study of loess-soil series, it allows recognition of subaerial processes which contributed to the accumulation of loess horizons between the stages of soil formation.

Samples were treated using the procedure developed by the Institute of Geography, Russian Academy of Sciences research group (Velichko and Timireva, 1995). Quartz sand grains of two size groups, 0.5–1.0 and 1.0–2.0 mm (50 grains from each fraction), were studied for grain surface texture and roundness.

Quartz grains from the Tiraspolian sand (unit 22) have the highest roundness coefficient (69–70%) and the lowest degree of dullness (6–7%). Glossy well-rounded grains (roundness class III) are dominant (Fig. 9). The grain

surfaces bear distinctive traces of water reworking, including small narrow V-shaped furrows indicative of prolonged processing in a highly dynamic medium (Fig. 10).

Quartz grains from the overlying Vorona palaeosol complex (PC 4) are quite different. The grains belong mostly to classes II and III, and the proportion of moderately rounded grains is rather high. Grains with traces of modification by water are rather common. The dominant features of the grain surface texture are those resulting from intense chemical weathering processes, including U-shaped grooves and secondary quartz formation (mostly within hollows on the grain surfaces). The roundness coefficient is considerably less than in samples from the Tiraspolian sand (61.5%). A sizeable group of partially matted grains bearing traces of aeolian abrasion (micro-pits) is present. The degree of matting reaches 32%, compared with the underlying Tiraspolian sands,

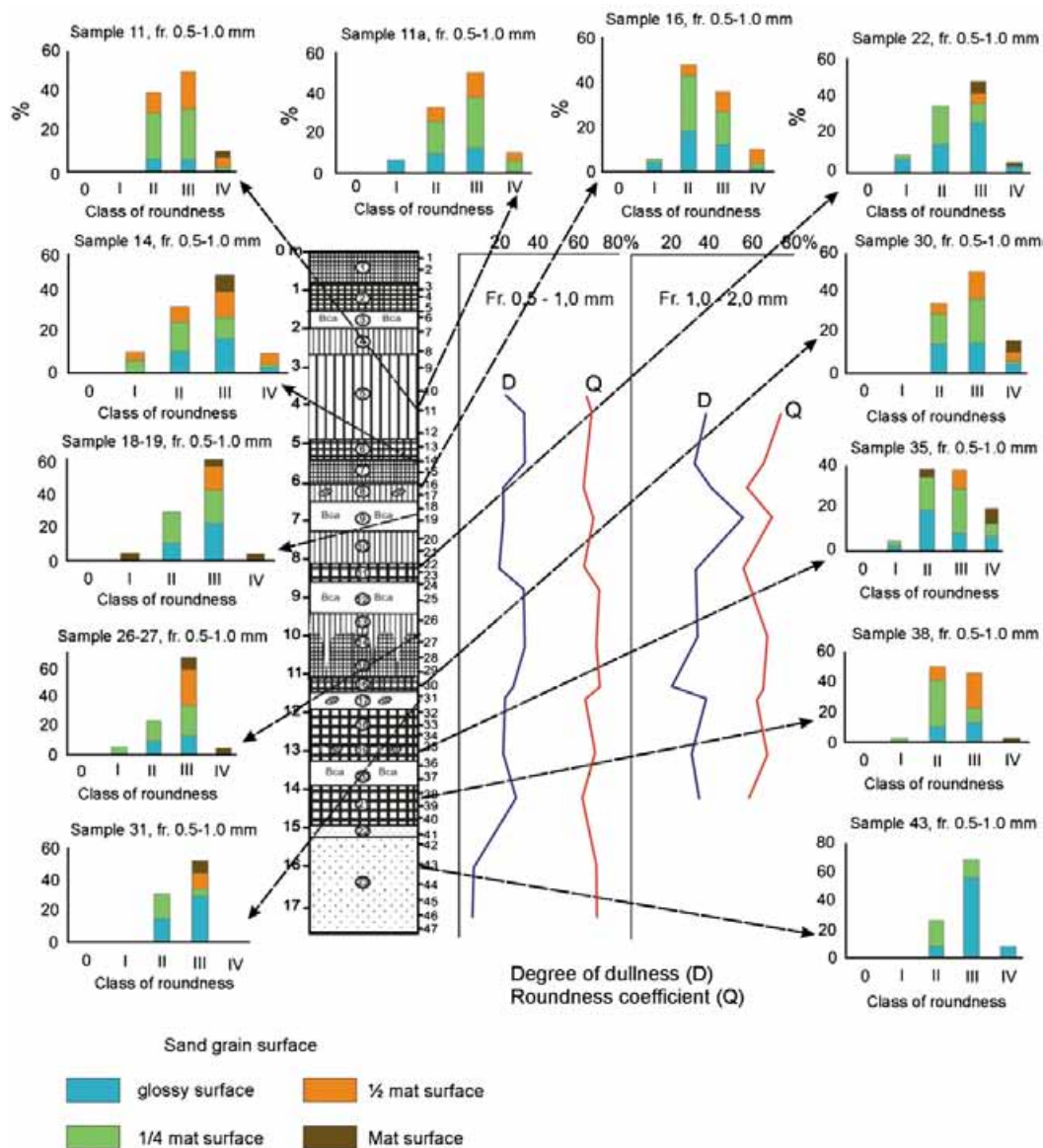


Fig. 9. Morphoscopy of quartz sand grains.

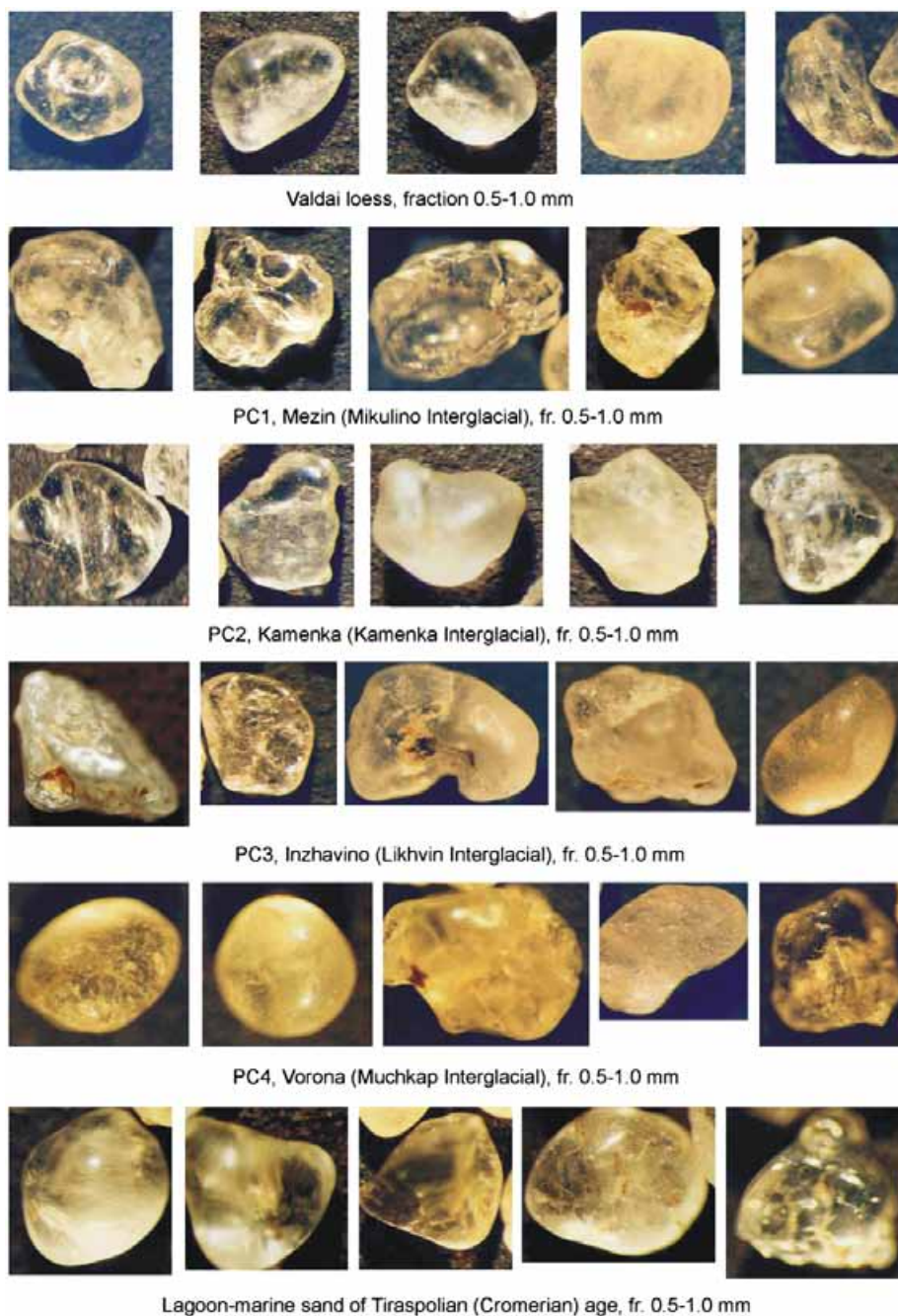


Fig. 10. Quartz sand grains from Semibalki-1 section (original magnification $\times 6.25$).

suggesting rather active aeolian processes at the time of sedimentation. Subsequently, in the process of soil development, the sand grains were subjected to soil-forming processes and acquired features typical of soil horizons. Sand grain morphoscopy suggests that the environments of soil formation were humid and warm, and, therefore, favourable for active chemical processes.

A steady increase in the degree of matting (from 24% to 36%) and roundness coefficient (64.5–69.5%) is evident within the Inzhavino palaeosol complex, PC 3. The degree of matting increases at a slightly greater rate than does roundness. It seems likely that aeolian activity was rather

high at the time of deposition. The data obtained are in reasonable agreement with results of earlier investigations (Velichko et al., 1997). Apparently, it takes less time for the grain surface to acquire a specific texture due to aeolian abrasion (matting) than to be rounded.

Common to most of the samples is the predominance of well-rounded grains (class III), with noticeable concentrations of moderately rounded ones (class II). There is also an increase in the amount of perfectly rounded grains in the upper portion of the sequence. Most grains show some evidence of matting. Genetically, all the grains are attributable to two main groups: fluvial, with glossy,

well-rounded grains, and aeolian grains with dull-smoothed surfaces and micro-pits. However, grain transportation in air was not prolonged, as the grains show a relatively low degree of matting, with glossy and quarter-matted surfaces prevailing. The grain surfaces were also affected by chemical weathering. The processes resulted in partial dissolution and deposition of quartz, the deposition being mostly restricted to negative microforms on the grain surface.

The Kamenka palaeosol complex (unit 11) has a considerably lesser degree of matting (20% maximum) and a somewhat lower roundness coefficient, to a maximum of 63%. Most grains belong to classes II and III, with a negligible amount of perfectly and very poorly rounded grains. In addition to grains of fluvial and aeolian origin, there are scattered examples seemingly bearing traces of seasonal or diurnal freezing (triangular hollows, fresh conchoidal fractures) and chemical weathering (scaly surfaces with V-shaped furrows).

The overlying Bca unit (9) of the Mezin complex does not display any essential difference from the lower units of the Kamenka palaeosol complex PC 2, except for slightly higher values of matting and roundness (by ~3.5%). The proportion of grains belonging to roundness class III reaches its peak in this unit. Most grains have glossy or quarter-matted surfaces, although some are completely matted. The roundness coefficient averages 66.5%, and the modal matting degree is 23.5%. The sample contains some grains with pitted or scaly surfaces, with traces of secondary quartz deposition. It seems probable that these elements resulted from chemical processes in the soils. Many grains seem to be waterworn (glossy or quarter-matted grains, rounded or smoothed), as well as bearing faint (seemingly initial) traces of aeolian abrasion. The latter occur mostly on prominent elements of grain surfaces.

The AB horizon, unit 8, is similar to those from the underlying units in the genetic characteristics of the sand grains. It contains grains carrying traces of fluvial and weak aeolian processes, as well as those of chemical weathering. The latter was likely more active, as indicated by numerous grains with pitted corroded surfaces. As well, there are numerous grains with conchoidal fractures which could be the results of frost weathering. The roundness coefficient of grains is 62.5%, and the dominant roundness classes are II and III, with class II being slightly more abundant. The great majority of grains feature glossy and quarter-matted surfaces, and the degree of matting is about 21.5%.

The grain characteristics are somewhat different in the Salyn palaeosol (unit 7). Although the roundness is practically the same as in the underlying unit, the degree of matting increases by more than 10% and amounts to 32% in the 0.5–1 mm fraction. The proportion of completely matted grains is 10%, which suggests a slightly higher intensity of aeolian processes. Soil-forming processes and frost weathering seem to also have been active,

as indicated by a higher amount of grains with small conchoidal fractures, crescent-shaped furrows, and secondary quartz formations.

Analysis of sand grains from the Valdai loess (unit 5) has shown their roundness and degree of matting to be among the highest within the sequence (67.5% and 32.5%, respectively). Most grains show evidence of fluvial abrasion. Subsequent aeolian abrasion varies widely in degree. Many grains have almost glossy surfaces, which hardly show any traces of wind action. Equally numerous are grains with pronounced traces of wind abrasion—well rounded, matted or half-matted surfaces with micro-pits. Some grains bear signs of frost weathering (small fresh fractures and triangular hollows).

The most distinct traces of frost weathering are found in the overlying horizon (unit 4), where a considerable number of grains have frost-induced features. Aeolian working is less pronounced than in the loess, fully matted grains are absent, and those with half-matted surfaces are reduced in number. The matting degree is reduced to 24%, and the roundness coefficient is about 66%.

The data suggest gradual changes in sedimentation environments from the base to the top of the sequence. The lower part of the sandy Tiraspolian (Cromerian) series was mostly deposited by water. The overlying units show evidence of more active aeolian processes and chemical weathering, while the uppermost part was deposited under the influence of aeolian and cryogenic processes. Accordingly, the degree of matting is minimal (6–7%) near the base of the sequence and reaches its maximum at the top (32.5%). The roundness coefficient values are rather high throughout the sequence (61.5–70%), with distinct peaks in the higher, middle, and lower parts.

6. Palynological analysis, upper part of the Semibalki sequence

Samples from the upper part of the Semibalki sequence have been studied palynologically. They permit only tentative conclusions on the quantitative relationship among the principal constituents of the spectra.

Pollen assemblages determined in unit 4 and the uppermost part of unit 5 (Valdai loess) are dominated by non-arboreal constituents (NAP) (Fig. 8). Typically for steppe assemblages, they abound in Chenopodiaceae, Gramineae, and *Artemisia*, including *Artemisia* s.gen. *Seriphidium*. Cichoriaceae pollen constitutes a noticeable portion of the assemblages. These typical inhabitants of disturbed grounds grew presumably on the coastal scarp and could occur on the adjacent flat surface with scarce vegetation.

In the lower part of unit 5, there is a noticeable rise (up to 40%) in AP abundance, mostly *Pinus sylvestris*, with individual grains of *Picea* and *Betula*. The proportion of Cichoriaceae and *Artemisia* is high. It is not inconceivable that some open forest communities did exist in the region at that time, giving a forest-steppe appearance to the environment. This could be related to the Mid-Valdai

mega-interstadial (MIS 3). However, the data at hand do not permit a definite conclusion on this point. *Pinus* pollen can be easily transported by wind for tens of kilometres, and no plants that could be confidently attributed to a forest floristic complex has been found among the NAP. The problem requires future investigations.

The upper part of the Mezin palaeosol complex (unit 6) yielded pollen assemblages not unlike those of unit 4, except for a somewhat higher content of Chenopodiaceae. The assemblage is definitely representative of a steppe environment.

Pollen spectra recovered from the lower humic horizon of PC 1 (Salyn, unit 7) are distinguished by considerably higher percentages of AP (up to 65%), with dominance of *Pinus* and *Betula* and small proportions of *Ulmus* and *Acer*. In the NAP group, *Artemisia* and Gramineae prevail, while Cichoriaceae participation is considerably reduced. The pollen assemblages are indicative of forest-steppe communities over the region at that time, and the presence of themophilic tree species (*Ulmus*, *Acer*) suggests interglacial environments.

Pollen assemblages of unit 8 are noticeably different from those of the overlying unit. The proportion of NAP rises to 93%. The assemblages are dominated by *Artemisia*, with Gramineae, Chenopodiaceae, Asteraceae, and Cichoriaceae present in small amounts. The vegetation was similar to the modern southern steppe.

7. Magnetic susceptibility

The magnetic susceptibility (K) varies through the sequence from 34 to 952×10^{-3} SI-units/g. Maximum K values are found in soils: $K_{max} = 344 \times 10^{-3}$ SI-units/g in the modern soil, 522×10^{-3} SI-units/g in the Mezin palaeosol, 466×10^{-3} SI-units/g in the Kamenka palaeosol, and 952×10^{-3} SI-units/g in the Vorona palaeosol. A rather low value of magnetic susceptibility is recorded in the Inzhavino palaeosol: $K_{max} = 176 \times 10^{-3}$ SI-units/g. Lower values were noted in loess horizons separating the palaeosols, and in layers below the Vorona palaeosol, ranging from 34 to 102×10^{-3} SI-units/g.

The palaeosols studied in the Semibalki-1 section have higher magnetic susceptibility as compared with the intervening units. The peaks are conspicuous in the general curve of susceptibility changes with depth, and the curve itself has a complicated (“sawtooth”) character. From the maximum value in the Vorona PC, the K value drops to 42×10^{-3} SI-units/g in the loess separating Vorona and Inzhavino PCs. The Inzhavino PC, although having lower K values than other palaeosols studied in the section and than the modern soil, still exceeds both overlying and underlying loess horizons in magnetic susceptibility.

There is a noticeable growth of K value within the two younger palaeosols. In the Kamenka PC, K changes from the base upwards as follows: 446; 151; 191; and 94×10^{-3} SI-units/g. Quite comparable growth of K (though with a greater maximum) has been recorded in the Mezin PC: 163;

522; 381; and 98×10^{-3} SI-units/g. In the modern soil K value changes from the base to the top as follows: 120; 344; and 118×10^{-3} SI-units/g (see Fig. 7).

The magnetic susceptibility data of the series exposed in the Semibalki-1 section indicates that the environments of soil formation promoted generation of pedogenic superparamagnetic magnetite, known to be the carrier of magnetic properties in fossil soils of Central Asia, China, and Africa (Heller and Liu, 1984; Liu et al., 1988; Heller et al., 1991). The variations of magnetic susceptibility follow the “Chinese” pattern, with K being essentially higher in palaeosols in comparison with underlying loess horizons.

8. Isotopic studies

Isotope analysis of oxygen ($\delta^{18}\text{O}$) and carbon ($\delta^{13}\text{C}$) was applied to carbonates and humus of the palaeosols sampled in the Semibalki-1 section. Carbonates are found in palaeosols and loess either as lime nodules (“byeloglazka”), or as mycelium, or as dispersed carbonate particles. Nine samples of palaeosol humus have been analysed for oxygen isotopes and 5 samples of carbonates derived from palaeosols and loess were analysed for oxygen and carbon isotopes. In addition, some thin sections prepared from samples of palaeosols and loesses proved to contain included grains of primary limestone. These lithogenic impurities prevent the use of carbonates from those palaeosols for reconstructions based on carbon isotopes in 2 out of 5 carbonate samples taken from the Semibalki-1 section). The preliminary results are presented in Fig. 7.

9. Small mammal fauna

Washing of sediments filling krotovinas revealed high concentrations of small vertebrate remains in almost all of the palaeosol horizons. The richest material was recovered from the Vorona palaeosol (PC 4) overlying the Tiraspolian fluvial deposits. The horizon abounds in krotovinas, most probably left by *Spermophilus* sp. Most commonly found are bones of long-clawed ground squirrels, *Spermophilus* sp. Less abundant are yellow steppe lemming (*Eolagurus* cf. *luteus*), steppe lemming (*Lagurus lagurus*), and common vole (*Microtus* sp.).

Scarcity of identifiable bone remains does not allow a definite conclusion about the age of the assemblage. All the mammals are represented by taxa characteristic for the Middle–Late Pleistocene and Holocene of Eastern Europe.

The assemblage includes mostly inhabitants of open landscapes and various semi-closed biotopes. Modern ground squirrels live in open steppe biotopes, steppe lemmings in forest-steppe, steppe, and semi-deserts, and yellow steppe lemmings in dry steppe and semi-deserts. On the whole, the fauna suggests a drier climate at the time of the formation of the Vorona palaeosol than that of today’s faunal assemblage. It seems conceivable that the

taphocoenosis was formed on steppe and forest-steppe slopes of the Don River valley.

The younger palaeosols also evolved under rather dry conditions of steppe and forest-steppe. Compositions of mammal assemblages were much the same through the Late Pleistocene. Taken as a whole, the relatively limited and taxa-conservative small mammal faunal assemblages, largely identified only to genus level, do not provide definitive evidence of a significant shift in climate. The modern faunal assemblage may in part reflect the altered availability of food resources and water due to human agricultural activity.

10. Conclusion

The subaerial succession exposed in the Semibalki-1 section overlies lagoonal-marine sediments dated to the Tiraspolian (Cromerian), latest Early Pleistocene. There are four palaeosol complexes identified within the series. The soils developed on terrestrial loess deposits. General data on humus and carbonate content confirm the presence of several levels marked by activated soil-forming processes. The same processes are reflected in magnetic susceptibility measurements.

Chronostratigraphic setting of the identified units has been ascertained using data on fossil small mammal fauna. The onset of soil formation in the subaerial succession postdates the Tiraspolian faunal assemblage.

The integrated data of paleopedological analysis (including studies of thin sections prepared from various genetic horizons of palaeosols) allowed analysis of the palaeosols. They are correlated with the principal Middle

and Late Pleistocene interglacial stages using the morphotypical characteristics developed for different-aged palaeosols of the East European Plain. The age of the lower Vorona and Inzhavino palaeosols, however, should be considered as tentative. Further investigations of small mammal fauna and numerical dating would be useful.

The earliest palaeosol complex in the Semibalki-1 section is correlated with the late Muchkap Interglacial (the Vorona palaeosol). The soil type was close to that of the modern subtropical semi-humid Mediterranean region soils. The later Middle Pleistocene palaeosols bear evidence of soil-forming processes typical of various temperate zone environments. Soils similar to prairie chernozems developed during the Likhvin Interglacial (Inzhavino PC), although the upper parts of the pedocomplex suggest a transition to semi-humid conditions, with kastenozemic development and increased ferruginization. PC 2 (Kamenka Interglacial) is typified by eluviated luvisc chernozem soils, with some elements associated with brown forest-fringe luvisols, suggesting formation under somewhat cooler and drier conditions than the preceding Inzhavino pedocomplex. Finally, the Mikulino Interglacial of the Late Pleistocene (Mezin PC) is represented by chernozems similar to modern (Holocene) soils of the region, but with less evidence of seasonal frost action and some podzolization Fig. 11.

The data may be summarized as follows: a succession of environmental changes has been traced in the study region, from semi-humid subtropical Mediterranean environments during the Muchkap Interglacial (Vorona Pedocomplex, PC 4), to temperate during the Likhvin Interglacial (Inzhavino Pedocomplex, PC 3), then to boreal-temperate transitional during the Kamenka Interglacial (PC 2), and

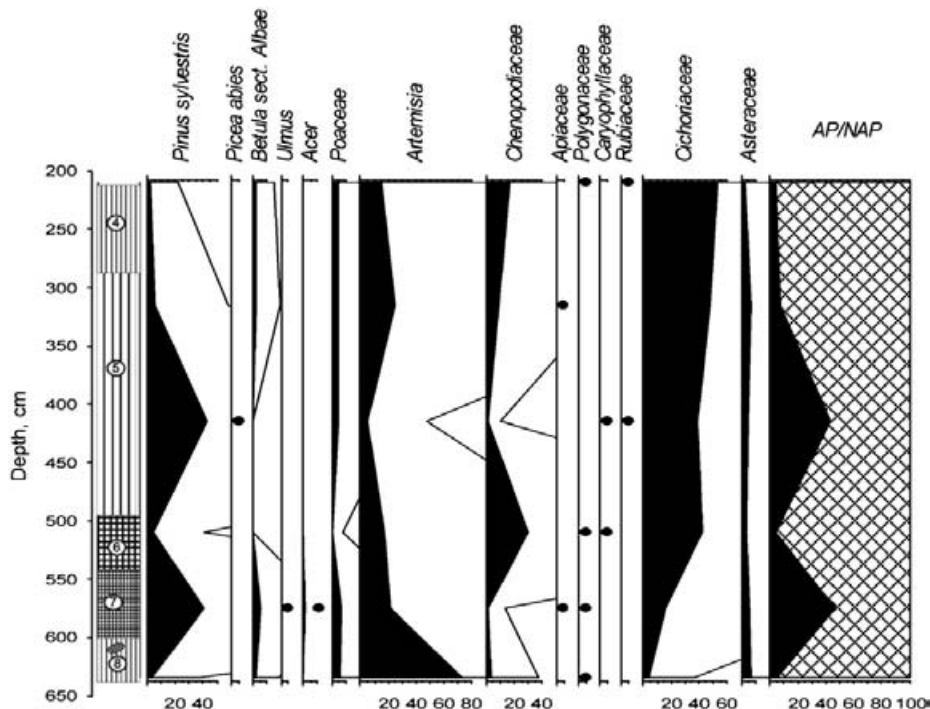


Fig. 11. Pollen diagram of the upper part of Semibalki-1 section.

Soil Complex	Soil types				
	<i>Chernozem (with frost features; normal or micelar)</i>	<i>Chernozem (leached and podzolized)</i>	<i>Eluviated Luvic Chernozem</i>	<i>Eluviated Chernozem- Kastenzem</i>	<i>Semihumid Subtropical soil</i>
<i>Contemporary (Holocene)</i>					
<i>PC1 Mikulino Interglacial</i>					
<i>PC2 Kamenka Interglacial</i>					
<i>PC3 Likhvin Interglacial</i>					
<i>PC4 Muchkap Interglacial</i>					

Fig. 12. Progressive shift of types of soil-forming processes with time.

finally towards landscapes with typical steppe soils in the Mukulino Interglacial (Mezin Pedocomplex, PC 1), and Holocene (Fig. 12). The sequence indicates that moisture supply and temperatures during successive interglacials shifted progressively towards increasingly cooler, somewhat drier climates, influencing soil formation.

Acknowledgments

We gratefully acknowledge the thorough reviews of the initial version of our manuscript by Natalia Gerasimenko and Slobodan Markovic, which resulted insubstantial improvements to the final text. Financial support for this research was provided by the Russian Academy of Sciences and by the Natural Sciences and Engineering Research Council of Canada.

References

- Agadjanian, A.K., Dobrodeev, O.P., Kursalova, V.I., Motusko, A.N., 1972. Paleofaunistic characteristic of a key section in the Azov region near Veselo–Voznesensky village. In: Nikolaev, N.I., Naimark, A.A. (Eds.), Neotectonics, Cenozoic Deposits and Man (in Russian).
- Bolikhovskaya, N.S., Dobrodeev, O.P., 1972. Paleogeography of the Pleistocene in the Azov region based on the data of pollen assemblages and Palaeosol studies of the Veselo–Voznesensky section. In: Nikolaev, N.I., Naimark, A.A. (Eds.), Neotectonics, Cenozoic Deposits and Man (in Russian).
- Dlussky, K.G., 2001. Srednepleistotsenovoye pochvoobrazovanie tsentra Vostochno-Evropetskoi Ravniny [Ph.D. thesis], Moscow, Russian Academy of Sciences, Institute of Geography, p. 250 (in Russian).
- Dlussky, K.G., 2007. Likhvin interglacial polygenetic Palaeosol: A reconstruction on the Russian Plain. *Quaternary International* 162–163, 141–157.
- Dodonov, A.E., Sadchikova, T.A., Tesakov, A.S., Titov, V.V., Trubikhin, V.M., 2005. Stratigraphic problems of Pleistocene–Quaternary covering formations of the North Eastern coasts of the black sea and the Azov region. In: Proceedings of International Conference on Problems of Paleontology and Archeology of the South of Russia and Adjoining Territories. Rostov-na-Donu, pp. 26–28 (in Russian).
- Gromov, V.I., 1933. Studies of the Quaternary fauna of the northern caucasus. *Vestnik Akademii Nauk* 4, 21–29 (in Russian).
- Heller, F., Liu, Tungsheng, 1984. Magnetism of Chinese loess deposits. *Geophysical Journal of the Royal Astronomical Society* 77, 125–141.
- Heller, F., Liu, X.M., Liu, T.S., Xu, T.S., 1991. Magnetic susceptibility of loess in China. *Earth and Planetary Science Letters* 103, 301–310.
- Khokhlovkina, V.A., 1940. Terraces of the Azov coast between Rostov and Taganrog cities. *Proceedings of the Institute of Geological Sciences (the USSR Academy of Sciences), Geological Series* 8 (28), 71–89 (in Russian).
- Lebedeva, N.A., 1965. Geological setting of small mammal sites in the Anthropogene of the Azov region. In: Stratigraphic importance of the Anthropogene fauna of small mammals. Nauka Press, Moscow, pp. 11–140 (in Russian).
- Lisitsyn, K.I., 1925. Geological setting of the planned channel route in the Don River delta and at the Taganrog Bay Southern Coast. p. 42 (in Russian).
- Little, E.C., 2002. Sedimentology and stratigraphy for Quaternary deposits of the Russian Plain [Ph.D. thesis], University of Alberta, Edmonton, Canada, p. 272.
- Little, E.C., Lian, O.B., Velichko, A.A., Morozova, T.D., Nechaev, V.P., Dlussky, K.G., Rutter, N.W., 2002. Quaternary stratigraphy and optical dating of loess from the East European Plain (Russia). *Quaternary Science Reviews* 21, 1745–1762.
- Liu, X., Xu, T., Liu, T., 1988. The Chinese loess in Xifeng. *Geophysical Journal* 92, 349–353.
- Morozova, T.D., 1981. Evolution of Soils in Europe during the Late Pleistocene. Nauka Press, Moscow, p. 282 (in Russian).
- Moskvitin, A.I., 1932. Quaternary deposits in the vicinities of Taganrog. In: Guidebook of the 2nd Quaternary Geological Conference. The USSR Academy of Sciences Press, Moscow-Leningrad, pp. 35–38 (in Russian).
- Puterbaugh, J., Catto, N.R., Velichko, A.A., Matishov, G.G., Morozova, V.P., Nechaev, V.P., Novenko, E.Y., Sumborski, T.V., Timireva, S.N., Rutter, N.W., Evans, M.E., 2005. Progressive shifts in interglacial climates, Don River Basin-Sea of Azov, Russia. Canadian Quaternary Association biennial meeting, Winnipeg, Canada, Abstract, A72.
- Velichko, A.A., 1990. Loess-paleosol formation on the Russian Plain. *Quaternary International* 7/8, 103–114.
- Velichko, A.A., Morozova, T.D., Pevzner, M.A., 1973. Structure and age of loess and palaeosol horizons on the main terraces in the Northern Azov region. In: Analysis of Paleomagnetism in Quaternary Deposits and Volcanic Studies. Nauka, Moscow, pp. 48–70 (in Russian).
- Velichko, A.A., Gribchenko, Yu.N., Timireva, S.N., 1997. Modelling of eolian processing of sand grains. *Litologiya i Poleznye Iskopaemye* 4, 431–439 (in Russian).
- Velichko, A.A., Akhlestina, E.F., Borisova, O.K., Gribchenko, Y.N., Zhidovinov, N.Y., 1999. East European Plain. In: Velichko, A.A., Nechaev, V.P. (Eds.), Climate and Environmental Changes during

- the Last 65 Million Years. GEOS, Moscow, pp. 43–83 Chapter. 3, (in Russian).
- Velichko, A.A., Morozova, T.D., Timireva, S.N., Nechaev, B.P., Panin, P.G., Novenko, E.Yu., 2005. Evolution of soils and subaerial processes during the Pleistocene in the central and southern regions of the East European Plain. In: Proceedings of International Conference on Problems of Paleontology and Archeology of the South of Russia and Adjoining Territories, Rostov-na-Donu, (in Russian), pp. 11–12.
- Velichko, A.A., Morozova, T.D., Nechaev, V.P., Rutter, N.W., Dlusskii, K.G., Little, E.C., Catto, N.R., Semenov, V.V., Evans, M.E., 2006a. Loess/paleosol/cryogenic formation and structure near the northern limit of loess deposition, East European Plain, Russia. *Quaternary International* 152/153, 14–30.
- Velichko, A.A., Semenov, V.V., Pospelova, G.A., Morozova, T.D., Nechaev, V.P., Gribchenko, Y.N., Dlusskii, K.G., Rutter, N.W., Catto, N.R., Little, E.C., 2006b. Matuyama-brunhes boundary in key sections of the loess-paleosol-glacial formations on the East European Plain. *Quaternary International* 152/153, 94–102.
- Velichko, A.A., Timireva, S.N., 1995. Morphoscopy and morphometry of quartz grains from loess and buried soil layers. *Geological Journal* 36 (2/3), 143–149.